

**SYNTHESIS AND CHARACTERIZATION OF
pH-SENSITIVE POLYELECTROLYTE
NANOGEELS FOR ORAL DELIVERY OF BOVINE
SERUM ALBUMIN AND INSULIN AS MODEL
PROTEINS**

by

JAHANZEB MUDASSIR

Thesis submitted in fulfillment of the requirements

for the Degree of

Doctor of Philosophy

February 2018

ACKNOWLEDGEMENT

Bismillah-hi-Rahma-ni-Raheem

Alhamdolillah-e-Rabb-el-Aalameen

First of all, all praises be to The Allah Almighty, The Exalted, The Most Gracious and Most Merciful. I also sends “Darud and Salam” to the Holy Prophet Muhammad (Peace of Allah be Upon Him). It is pleasure to thank The Allah Almighty, The creator of universe, Who is The Supreme behind successful completion of my PhD studies.

I would like to express my utmost gratitude and appreciation to my dedicated Supervisor Assoc. Prof. Dr. Yusrida Darwis who has supported me with all her mentorship and guidance throughout my research. A few of her excellent qualities include her continuous contact and communication with students, prompt response when we contacted her, frequent meetings with students, lab visits, her concerns and worries for the student and immediate action she takes to solve the problem of her students. I also gratefully acknowledge my Co-supervisor Prof. Dr. Peh Kok Khiang. He was always encouraging and helpful.

I would like to express my sincere thanks to Institute of Post-Graduate studies (IPS) for providing me with USM fellowship. I would like to thank USM for providing all necessary facilities that made study possible.

I would like to thank all members of my family for their love, prayers and support throughout my whole life. I dedicate achievements to my beloved parents. I am blessed to have such an affectionate and courageous Father and Mother (Alhamdulillah). Due to their prayers, I have never seen difficult time in my life. I also want to thank my wife (Sibgha Naz Khan), love and prayers for my beloved

daughter (Eshal Jahanzeb) and son (Muhammad Shazil Khan) who gave me all their love and support. Without which my Ph.D. life would not have been so joyful in Penang, Malaysia.

The completion of this project may not be possible without the help from the laboratory staff in discipline of Pharmaceutical Technology especially Mr. Samsudin Bakar, Mr. Ibrahim Zainal Abidin, and Mr. Mohd Hafiz Abdul Rahim. Besides I am also grateful towards Mr. Roseli Hassan for their technical support in the animal study.

I am really thankful to all my fellow lab mates especially Mrs Ang Lee Fung, Mrs Noratiqah Binti Mohtar, Mr. Ibrahim M Abdulbaqi, Mrs. Reem Abou Assi, and Mr. Arshad A Khan for their help, moral support and scientific discussion.

Jahanzeb Mudassir

TABLE OF CONTENTS

ACKNOWLEDGEMENT	ii
TABLE OF CONTENTS	iv
LIST OF TABLES	xviii
LIST OF FIGURES	xxi
LIST OF PLATES	xxvi
LIST OF ABBREVIATIONS AND SYMBOLS	xxvii
ABSTRAK	xxxii
ABSTRACT	xxxv
 CHAPTER 1: INTRODUCTION	
1.1 Peptide and protein therapeutics	1
1.1.1 Current routes of peptide and protein administrations and limitations	2
1.2 Challenges in oral peptide and protein delivery	3
1.2.1 Critical issues with physicochemical properties of peptide and protein	3
1.2.2 <i>In vivo</i> barriers associated with oral peptide and protein delivery	3
1.3 Transportation of peptide and protein and loaded nanocarriers across intestinal epithelium	5
1.3.1 Trans-cellular pathways	5
1.3.2 Para-cellular pathway	6
1.3.3 Specific uptake of ligand-modified nanocarriers	7
1.4 Approaches to overcome oral peptide and protein delivery barriers	8
1.4.1 Enteric coating	9

1.4.2	Permeation or absorption enhancers	9
1.4.3	Enzyme inhibitors	10
1.4.4	Physicochemical modification of peptide and protein	11
1.4.5	Muco-adhesive polymeric systems	12
1.4.6	Alternative approaches for enhancing the absorption of peptide and protein	13
1.5	Characteristics of ideal oral peptide and protein delivery systems	13
1.6	Oral peptide and protein delivery systems	14
1.6.1	Micro or nano-emulsions	14
1.6.2	Liposomes	15
1.6.3	Chitosan based nanoparticles	15
1.6.4	Poly (lactide-co-glycolide) (PLGA) nanoparticles	16
1.6.5	Nanogels (NGs)	17
1.7	Vinyl and acrylic based carriers for oral peptide and protein delivery	17
1.7.1	Polymers possessing pH-dependent swelling behaviour	18
1.7.2	Polymers possessing pH-responsive dissolution characteristics	18
1.7.3	Vinyl and acrylic based nanogels	19
1.7.4	Nanogels composition and synthesis	20
1.7.4(a)	Mass polymerization	21
1.7.4(b)	Solution polymerization	22
1.7.4(c)	Suspension polymerization	22
1.7.4(d)	Emulsion polymerization	22
1.7.5	Mechanism and characteristics of nanogels overcoming barriers to oral peptide and protein	23
1.7.5(a)	pH-sensitive nanogels	24

1.7.5(b)	Enzyme inhibition capability	25
1.7.5(c)	TJs opening capability (paracellular pathway)	27
1.7.5(d)	Non-destructive loading methods	28
1.8	Model protein drugs	29
1.8.1	Bovine Serum Albumin (BSA) as model protein	29
1.9	Insulin	33
1.9.1	Insulin discovery and structure	34
1.9.2	Diabetes and its prevalence	34
1.9.3	Technologies for oral delivery of insulin under investigations	36
1.9.4	Challenges and mechanism to overcome oral insulin delivery barriers using vinyl and acrylic based nanogels	36
1.9.5	Vinyl and acrylic based nanogels for oral insulin delivery	38
1.10	Statement of the problem	42
1.11	Objectives of present study	43
CHAPTER 2:	SYNTHESIS AND CHARACTERIZATION OF METHYL METHACRYLATE-CO-ITACONIC ACID-CL-ETHYLENE GLYCOL DIMETHACRYLATE (MMA/IA) NANOGELS	45
2.1	Introduction	45
2.2	Materials	47
2.3	Methods	48
2.3.1	Synthesis of methyl methacrylate-co-itaconic acid-cl-ethylene glycol dimethacrylate (MMA/IA) nanogels	48
2.3.2	Purification of nanogels	51
2.3.3	Determination of yield	52
2.3.4	Physicochemical characterizations of MMA/IA nanogels	52

2.3.4(a)	Fourier transform infrared (FTIR) spectroscopy analysis	52
2.3.4(b)	Proton nuclear magnetic resonance (^1H NMR) analysis	52
2.3.4(c)	Estimation of molecular weight using LC-TOF-MS	53
2.3.4(d)	X-ray diffractometer (XRD) analysis	53
2.3.4(e)	Transmission electron microscopy (TEM)	53
2.3.4(f)	Determination of particle size, polydispersity index (PdI) and zeta potential	53
2.3.5	Determination of isoelectric point (pI) using aqueous electrophoresis (auto-titration)	54
2.3.6	Swelling ratios of pH-sensitive nanogels using gravimetric method	54
2.3.7	Statistical analysis	55
2.4	Results and discussion	55
2.4.1	Synthesis of MMA/IA nanogels	55
2.4.1(a)	Optimization of ethanol/water ratios	55
2.4.1(b)	Optimization of ethanol/water volume	57
2.4.1(c)	Optimization of crosslinker EGDMA concentration	59
2.4.1(d)	Optimization of MMA/IA ratios	62
2.4.2	Physicochemical characterization of MMA/IA nanogels	65
2.4.2(a)	FTIR spectroscopy	65
2.4.2(b)	Proton nuclear magnetic resonance (^1H NMR) analysis	67
2.4.2(c)	Estimation of molecular weight using LC-TOF-MS	68
2.4.3	Determination of yield	69
2.4.4	X-Ray Diffractometry (XRD) analysis	70

2.4.5	Transmission electron microscopy (TEM)	71
2.4.6	Isoelectric point (pI)	72
2.4.7	Swelling ratios	73
2.5	Conclusion	76
 CHAPTER 3: <i>IN VITRO</i> AND <i>IN VIVO</i> TOXICOLOGICAL EVALUATION OF pH-SENSITIVE NANOGELS FOR ORAL DRUG DELIVERY		77
3.1	Introduction	77
3.2	Materials	79
3.3	Methods	79
3.3.1	<i>In vitro</i> toxicity studies	79
3.3.1(a)	Culture of caco-2 cells	79
3.3.1(b)	Cytotoxicity of nanogel using MTT assay	80
3.3.2	<i>In vivo</i> toxicity studies	81
3.3.2(a)	Limit test	81
3.3.2(b)	Pathological examinations	81
3.3.3	Statistical analysis	82
3.4	Results and discussion	83
3.4.1	<i>In vitro</i> cytotoxicity study	83
3.4.2	<i>In vivo</i> toxicity study	84
3.4.2(a)	Toxicity signs and symptoms	86
3.4.2(b)	Effect on hematological and biochemical parameters	87
3.4.2(c)	Necropsy and histopathology	89
3.5	Conclusion	93

CHAPTER 4: SELF-ASSEMBLED POLYELECTROLYTE NANOCOMPLEXES OF BOVINE SERUM ALBUMIN AND NANOGELS	94
4.1 Introduction	94
4.2 Materials	96
4.3 Methods	97
4.3.1 Preparation of MMA/IA nanogels	97
4.3.2 Determination of pI of BSA using aqueous electrophoresis (auto-titration)	97
4.3.3 Preparation of BSA/NGs-PEC	97
4.3.4 Quantification of BSA using Bradford protein assay	98
4.3.5 Optimization of BSA/NGs-PEC parameters	98
4.3.6 Characterization of BSA/NGs-PEC	100
4.3.6(a) Particle size and PDI	100
4.3.6(b) Zeta potential	101
4.3.6(c) Determination of percent entrapment efficiency (% EE), drug loading (% DL) and yield	101
4.3.7 <i>In vitro</i> release profiles of BSA from BSA/NGs-PEC	102
4.3.8 Statistical analysis	103
4.4 Results and discussion	103
4.4.1 Preparation of BSA/NGs-PEC	103
4.4.2 pI of BSA and nanogels using aqueous electrophoresis	104
4.4.3 Prediction of pH and mechanism of PEC between BSA and nanogels	105
4.4.4 Confirmation of BSA/NGs-PEC formation	107
4.4.5 Quantification of BSA by using the Bradford reagent assay	109
4.4.6 Optimization of BSA/NGs-PEC complex	110

4.4.6(a)	Effect of BSA:NGs ratios on BSA/NGs-PEC properties	110
4.4.6(b)	Effect of pH on BSA/NGs-PEC properties	113
4.4.6(c)	Effect of incubation time on BSA/NGs-PEC properties	117
4.4.6(d)	Effect of stirring rate on BSA/NGs-PEC properties	119
4.4.7	<i>In vitro</i> release profile of BSA from BSA/NGs-PEC	122
4.5	Conclusion	125
CHAPTER 5: LYOPHILIZATION OF SELECTED BSA/NGs-PEC AND STABILITY STUDIES		126
5.1	Introduction	126
5.2	Materials	127
5.3	Methods	127
5.3.1	Lyophilization of optimized BSA/NGs-PEC	127
5.3.1(a)	Reconstitution of lyophilized BSA/NGs-PEC	128
5.3.2	<i>In vitro</i> release profiles of BSA from lyophilized BSA/NGs-PEC	128
5.3.3	Characterization of lyophilized BSA/NGs-PEC	129
5.3.3(a)	Evaluation of primary structural integrity of BSA released from lyophilized BSA/NGs-PEC (SDS-PAGE)	129
5.3.3(b)	FTIR spectra	130
5.3.4	Electron microscopic examination	131
5.3.4(a)	Transmission electron microscope (TEM)	131
5.3.4(b)	Scanning electron microscope (SEM)	131
5.3.5	Stability studies on BSA/NGs-PEC liquid and lyophilized formulations	131

5.3.5(a)	Determination of BSA content from formulations during stability studies	132
5.3.6	Statistical analysis	132
5.4	Results and discussion	133
5.4.1	Lyophilization of BSA/NGs-PEC	133
5.4.1(a)	Physical appearance	134
5.4.2	Lyophilization of BSA/NGs-PEC without cryoprotectant	135
5.4.2(a)	Effect on particle size, PdI, zeta potential and entrapment	135
5.4.3	Lyophilization of BSA/NGs-PEC using mannitol and trehalose	135
5.4.3(a)	Effect of mannitol on particle size and PdI	136
5.4.3(b)	Effect of trehalose on particle size and PdI	136
5.4.3(c)	Effect of mannitol and trehalose on zeta potential and % EE	138
5.4.4	<i>In vitro</i> release study of lyophilized BSA/NGs-PEC	139
5.4.5	Characterization of lyophilized BSA/NGs-PEC	141
5.4.5(a)	FTIR spectra	141
5.4.5(b)	Integrity of BSA released from lyophilized BSA/NGs-PEC using SDS-PAGE	142
5.4.5(c)	TEM	144
5.4.5(d)	SEM	145
5.4.6	Stability studies on BSA/NGs-PEC liquid and lyophilized formulations	146
5.4.7	Stability of BSA/NGs-PEC liquid formulations (BF16) stored at $5\pm 3^{\circ}\text{C}$ and $25\pm 2^{\circ}\text{C}/75\pm 15\%\text{RH}$	147
5.4.7(a)	Particle size and PdI at $5\pm 3^{\circ}\text{C}$ and $25\pm 2^{\circ}\text{C}/75\pm 15\%\text{RH}$	147
5.4.7(b)	Zeta potential at $5\pm 3^{\circ}\text{C}$ and $25\pm 2^{\circ}\text{C}/75\pm 15\%\text{RH}$	148

5.4.7(c)	Percent BSA contents at $5\pm 3^{\circ}\text{C}$ and $25\pm 2^{\circ}\text{C}/75\pm 15\%\text{RH}$	148
5.4.7(d)	<i>In vitro</i> release profile of BSA from BSA/NGs-PEC liquid formulation (BF16) stored at $5\pm 3^{\circ}\text{C}$ in SGF and SIF media	150
5.4.7(e)	<i>In vitro</i> release profile of BSA from BSA/NGs-PEC liquid formulation (BF16) stored at $25\pm 2^{\circ}\text{C}/75\pm 15\%\text{RH}$ in SGF and SIF media	152
5.4.8	Stability of BSA/NGs-PEC lyophilized formulation (BF16-Tre2) stored at $5\pm 3^{\circ}\text{C}$ and $25\pm 2^{\circ}\text{C}/75\pm 15\%\text{RH}$	154
5.4.8(a)	Physical appearance of BSA/NGs-PEC lyophilized formulations at $5\pm 3^{\circ}\text{C}$ and $25\pm 2^{\circ}\text{C}/75\pm 15\%\text{RH}$	154
5.4.8(b)	Particle size and PDI at $5\pm 3^{\circ}\text{C}$ and $25\pm 2^{\circ}\text{C}/75\pm 15\%\text{RH}$	154
5.4.8(c)	Zeta potential at $5\pm 3^{\circ}\text{C}$ and $25\pm 2^{\circ}\text{C}/75\pm 15\%\text{RH}$	155
5.4.8(d)	Percent BSA contents at $5\pm 3^{\circ}\text{C}$ and $25\pm 2^{\circ}\text{C}/75\pm 15\%\text{RH}$	155
5.4.8(e)	<i>In vitro</i> release profile of BSA from the BF16-Tre2 formulation at $5\pm 3^{\circ}\text{C}$ in the SGF and SIF media	157
5.4.8(f)	<i>In vitro</i> release profile of BSA from the BF16-Tre2 formulation stored at $25\pm 2^{\circ}\text{C}/75\pm 15\%\text{RH}$ in SGF and SIF media	158
5.5	Conclusion	160
CHAPTER 6: VALIDATION OF RAPID RP-HPLC METHOD FOR DETERMINATION OF INSULIN		161
6.1	Introduction	161
6.2	Materials	162
6.3	Methods	163
6.3.1	RP-HPLC chromatographic system	163
6.3.2	Chromatographic conditions (Acidic analytical method for determination of insulin)	163

6.3.3	Preparation of stock and standard solutions	164
6.3.3(a)	Preparation of insulin stock	164
6.3.3(b)	Preparation of calibration standards	164
6.3.4	Method validation	164
6.3.4(a)	System suitability	164
6.3.4(b)	Specificity	165
6.3.4(c)	Linearity	165
6.3.4(d)	Limit of detection and limit of quantification	166
6.3.4(e)	Intra-day and inter-day precision and accuracy	166
6.3.4(f)	Robustness	167
6.3.4(g)	Solution stability	167
6.3.5	Statistical analysis	167
6.4	Results and discussion	167
6.4.1	Method validation and optimization	167
6.4.1(a)	System suitability	167
6.4.1(b)	Specificity	168
6.4.1(c)	Linearity	170
6.4.1(d)	Limit of detection and limit of quantification	171
6.4.1(e)	Intra-day and inter-day precision and accuracy	171
6.4.1(f)	Robustness	171
6.4.1(g)	Solution stability	173
6.5	Conclusion	174

CHAPTER 7: SELF-ASSEMBLED INSULIN AND NANOGELS POLYELECTROLYTE COMPLEX (INS/NGs-PEC) FOR ORAL INSULIN DELIVERY: PREPARATION AND IN VIVO EVALUATION	175
7.1 Introduction	175
7.2 Materials	177
7.3 Methods	177
7.3.1 Preparation of MMA/IA nanogels	177
7.3.2 Physical behavior of insulin at different pHs	177
7.3.3 Determination of isoelectric point (pI) of insulin and Ins/NGs-PEC using aqueous electrophoresis (auto-titration)	177
7.3.4 Preparation INs/NGs-PEC	178
7.3.5 Optimization of Ins/NGs-PEC parameters	178
7.3.6 Characterization of Ins/NGs-PEC	180
7.3.6(a) Particle size and PDI	180
7.3.6(b) Zeta potential measurement	180
7.3.6(c) Determination of entrapment efficiency, drug loading and yield	180
7.3.7 Lyophilisation of optimized Ins/NGs-PEC	182
7.3.7(a) Reconstitution of lyophilized Ins/NGs-PEC	182
7.3.8 <i>In vitro</i> release profiles of insulin from Ins/NGs-PEC liquid (InF-12) and lyophilized (InF-12-Tre2) formulations	182
7.3.9 Characterization of lyophilized Ins/NGs-PEC	183
7.3.9(a) Evaluation of primary structural integrity of insulin released from lyophilized Ins/NGs-PEC (SDS-Polyacrylamide Gel Electrophoresis (SDS-PAGE))	183
7.3.9(b) Fourier transform infrared (FTIR) spectra	184
7.3.9(c) Transmission electron microscope (TEM)	184

7.3.10	Stability studies on Ins/NGs-PEC liquid and lyophilized formulations	184
7.3.11	<i>In vivo</i> evaluation of insulin loaded nanogels for hypoglycemic effect	185
7.3.11(a)	Animals	185
7.3.11(b)	Induction of diabetes using streptozotocin (STZ)	185
7.3.11(c)	Study design	186
7.3.11(d)	Determination of blood glucose level using glucometer	187
7.3.11(e)	Determination of serum insulin level using ELISA	187
7.3.12	Statistical analysis	188
7.4	Results and discussion	188
7.4.1	Physical appearance and behavior of insulin at different pHs	188
7.4.2	Preparation of INs/NGs-PEC	189
7.4.2(a)	Isoelectric point (pI) of insulin and nanogels using aqueous electrophoresis	190
7.4.2(b)	Prediction pH range for INs/NGs-PEC formation	190
7.4.2(c)	Mechanism of INs/NGs-PEC formation	191
7.4.2(d)	Confirmation of INs/NGs-PEC formation	193
7.4.3	Optimization of Ins/NGs-PEC complex	195
7.4.3(a)	Effect of Ins:NGs ratios on Ins/NGs-PEC properties	195
7.4.3(b)	Effect of pH on Ins/NGs-PEC properties	199
7.4.3(c)	Effect of incubation time on Ins/NGs-PEC properties	203
7.4.3(d)	Effect of stirring rate on Ins/NGs-PEC properties	205

7.4.4	<i>In vitro</i> release profile of insulin from Ins/NGs-PEC (InF12)	208
7.4.5	Lyophilisation of Ins/NGs-PEC (InF-12)	211
7.4.6	<i>In vitro</i> release study of lyophilized Ins/NG-PEC (InF12-Tre2)	213
7.4.7	Characterization of lyophilized Ins/NGs-PEC (InF12-Tre2)	214
7.4.7(a)	Fourier transform infrared (FTIR) spectra	214
7.4.7(b)	Integrity of insulin released from Ins/NGs-PEC (InF12-Tre2) using SDS-PAGE	215
7.4.7(c)	Transmission electron microscopy (TEM)	217
7.4.8	Stability studies on Ins/NGs-PEC liquid and lyophilized formulations	218
7.4.9	Stability of Ins/NGs-PEC liquid formulations (InF12)	219
7.4.9(a)	Particle size and PdI at $5\pm 3^{\circ}\text{C}$ and $25\pm 2^{\circ}\text{C}/75\pm 15\%\text{RH}$	219
7.4.9(b)	Zeta potential at $5\pm 3^{\circ}\text{C}$ and $25\pm 2^{\circ}\text{C}/75\pm 15\%\text{RH}$	220
7.4.9(c)	Percent insulin contents at $5\pm 3^{\circ}\text{C}$ and $25\pm 2^{\circ}\text{C}/75\pm 15\%\text{RH}$	220
7.4.9(d)	<i>In vitro</i> insulin release profile of InF12 formulation at stored at $5\pm 3^{\circ}\text{C}$ in SGF and SIF	221
7.4.9(e)	<i>In vitro</i> insulin release profile InF12 formulation stored at $25\pm 2^{\circ}\text{C}/75\pm 15\%\text{RH}$ in SGF and SIF	223
7.4.10	Stability of Ins/NGs-PEC lyophilized formulations (InF12-Tre2)	224
7.4.10(a)	Physical appearance of Ins/NGs-PEC lyophilized formulations (InF12-Tre2) at $5\pm 3^{\circ}\text{C}$ and $25\pm 2^{\circ}\text{C}/75\pm 15\%\text{RH}$	225
7.4.10(b)	Particle size and PdI at $5\pm 3^{\circ}\text{C}$ and $25\pm 2^{\circ}\text{C}/75\pm 15\%\text{RH}$	225
7.4.10(c)	Zeta potential at $5\pm 3^{\circ}\text{C}$ and $25\pm 2^{\circ}\text{C}/75\pm 15\%\text{RH}$	226
7.4.10(d)	Percent insulin contents at $5\pm 3^{\circ}\text{C}$ and $25\pm 2^{\circ}\text{C}/75\pm 15\%\text{RH}$	226

7.4.10(e)	<i>In vitro</i> insulin release profiles of InF12-Tre2 at formulation stored at $5\pm 3^{\circ}\text{C}$ in SGF and SIF	228
7.4.10(f)	<i>In vitro</i> insulin release profile of InF12-Tre2 formulation stored at $25\pm 2^{\circ}\text{C}/75\pm 15\%\text{RH}$ in SGF and SIF	229
7.4.11	<i>In vivo</i> evaluation of lyophilized insulin loaded nanogels (InF12-Tre2) for oral hypoglycemic effect	230
7.4.11(a)	Determination of blood glucose level	230
7.4.11(b)	Determination of serum insulin level in diabetic rats	235
7.5	Conclusion	238
CHAPTER 8:	CONCLUSION	239
CHAPTER 9:	SUGGESTIONS FOR FUTURE RESEARCH	242
REFERENCES		245

LIST OF TABLES

		Page
Table 1.1	Technologies for oral delivery of insulin under investigations	36
Table 2.1	Parameters investigated in the optimization of MMA/IA nanogels synthesis	49
Table 2.2	Optimization of parameters in MMA/IA nanogels synthesis	50
Table 2.3	Opt-I: The effect of different ethanol/water ratios on particle size, PdI, zeta potential and swelling ratio	57
Table 2.4	Opt-II The effect of dilution volumes of ethanol/water on particle size, PdI, zeta potential and swelling ratio	59
Table 2.5	Opt-III: The effect of different concentrations of crosslinker EGDMA on particle size, PdI, zeta potential and swelling ratio	62
Table 2.6	Opt-IV The effect of MMA/IA ratios on particle size, PdI, zeta potential and swelling ratio	64
Table 2.7	The optimized parameters for synthesis of MMA/IA nanogels (S14) and the results of particle size, PdI, zeta potential and swelling ratio	64
Table 3.1	The effect of single oral dose of 2000 mg/kg body weight MMA/IA nanogel on body weight, toxic symptoms and internal organs of female rats	85
Table 3.2	Effect of single oral dose of 2000mg/kg body weight MMA/IA nanogels on short term (48 hours) and long term (in 14 days) mortality	85
Table 3.3	Summary of mortality results after 14 days of single oral dose of 2000mg/kg body weight MMA/IA nanogels	86
Table 3.4	The effect of single oral dose of 2000 mg/kg body weight MMA/IA nanogel on hematological parameters of untreated (control) and treated groups female Sprague Dawley rats 14 days after treatment.	87
Table 3.5	The effect of single oral dose of 2000 mg/kg body weight MMA/IA nanogel on biochemical parameters of untreated (control) and treated groups female Sprague Dawley rats 14 days after treatment.	88

Table 3.6	The effect of single oral dose of 2000 mg/kg body weight MMA/IA nanogel on relative organ weight (ROW) untreated (control) and treated groups female Sprague Dawley rats 14 days after treatment.	89
Table 4.1	Parameters investigated in the optimization of BSA/NGs-PEC	99
Table 4.2	Optimization of parameters in BSA/NGs-PEC formulations	99
Table 5.1	Storage conditions during stability studies of BSA/NGs-PEC liquid and lyophilized formulations	132
Table 5.2	Lyophilization of optimized formulation of BF16 and the effect of the addition of trehalose and mannitol as cryoprotectant	139
Table 5.3	The stability data of BF16 liquid formulations stored at $5\pm 3^{\circ}\text{C}$ for six months	149
Table 5.4	The stability data of BF16 liquid formulations stored at $25\pm 2^{\circ}\text{C}/75\pm 15\%\text{RH}$ for six months	149
Table 5.5	The stability data of BF16-Tre2 formulation stored at $5\pm 3^{\circ}\text{C}$ for six months	156
Table 5.6	The stability data of BF16-Tre2 formulation stored at $25\pm 2^{\circ}\text{C}/75\pm 15\%\text{RH}$ for six months	156
Table 6.1	System suitability parameters of insulin at 2 $\mu\text{g}/\text{ml}$.	168
Table 6.2	Calibration curve results for insulin	170
Table 6.3	Intra-day and inter-day precision and accuracy results for insulin	172
Table 6.4	Analysis of method robustness using insulin at concentration of 2 $\mu\text{g}/\text{ml}$	173
Table 6.5	Stability studies of insulin in mobile phase	174
Table 7.1	Parameters investigated in the optimization of Ins/NGs-PEC	179
Table 7.2	Optimization of parameters in Ins/NGs-PEC formulations	180
Table 7.3	Storage conditions during stability studies of Ins/NGs-PEC liquid (InF12) and lyophilized (InF12-Tre2) formulations	185
Table 7.4	<i>In vivo</i> evaluation of optimized lyophilized insulin loaded nanogels formulations for oral hypoglycemic effect	187

Table 7.5	Lyophilization of optimized formulation of InF-12 with the addition of trehalose as cryoprotectant	212
Table 7.6	The stability data of InF12 liquid formulation stored at $5\pm 3^{\circ}\text{C}$.	221
Table 7.7	The stability data of InF12 liquid formulation stored at $25\pm 2^{\circ}\text{C}/75\pm 15\%\text{RH}$.	221
Table 7.8	The stability data of InF12-Tre2 lyophilized formulation stored at $5\pm 3^{\circ}\text{C}$	227
Table 7.9	The stability data of InF12-Tre2 lyophilized formulation stored at $25\pm 2^{\circ}\text{C}/75\pm 15\%\text{RH}$.	227

LIST OF FIGURES

		Page
Figure 1.1	An overview of three major <i>in vivo</i> barriers in oral Peptide and protein delivery	4
Figure 1.2	Intestinal barriers to Peptide and protein delivery (the intestinal epithelial barriers is composed of single layer of columnar epithelial cells and mucosal layer present on the apical side)	5
Figure 1.3	Transport mechanisms; (A) uptake of peptide and protein drugs across the intestinal epithelium; (B) transpotation of protein loaded nanoparticles through paracellular pathway	8
Figure 1.4	Characteristics of ideal DDS	14
Figure 1.5	Illustrative representation of the diversity of nanogels composition based on building components: (A) nanogels based on synthetic monomers or polymers; (B) based on natural monomers or polymers; (C) hybrid nanogels	21
Figure 1.6	Overview of mechanism of pH-sensitive nanogels to overcome major barriers	23
Figure 1.7	pH sensitive swelling behaviour of carboxylic acid groups containing nanogels	25
Figure 1.8	Illustration of mechanism of intestinal tight junction opening due the depletion of Ca^{++} ions by carboxylic acid functional groups containing nano-carriers.	28
Figure 1.9	Structure of (A) Human insulin, (B) Short acting insulin aspart	33
Figure 1.10	A flow chart of research activities	44
Figure 2.1	Structure of MMA, IA, EGDMA and MMA/IA nanogels	51
Figure 2.2	FTIR spectra of (A) MMA; (B) IA; (C) EGDMA and (D) non-dialysed MMA/IA nanogels (E) dialysed MMA/IA nanogels	66
Figure 2.3	^1H NMR spectra of (A) MMA; (B) IA; (C) EGDMA and (D) MMA/IA nanogels	68
Figure 2.4	LC-TOF-MS of pH-sensitive MMA/IA nanogels (A) chromatogram (B) TOF-MS spectrum	70
Figure 2.5	XRD pattern of pH-sensitive MMA/IA nanogels	71

Figure 2.6	Aqueous electrophoresis (auto titration) of pH-sensitive MMA/IA nanogels for determination of isoelectric point (pI)	73
Figure 2.7	Influence of various pHs i.e 1.2, 4.5, 6.8 and 7.4 on the swelling ratio of pH-sensitive MMA/IA nanogels as a function of time (upto 12 hours).	75
Figure 3.1	<i>In vitro</i> cytotoxicity of MMA/IA nanogel utilizing MTT assay The viability assay of Caco-2 cells using treatment (0.25, 0.5, and 1mg/ml nanogels) and control for 4 and 24 hours of incubation	84
Figure 4.1	Aqueous electrophoresis of BSA for determination of pI	105
Figure 4.2	Graphical illustration for the prediction of pH range of complex forming solution using the pI values of BSA and nanogels	106
Figure 4.3	Illustration of mechanism of PEC formation between BSA and nanogels	107
Figure 4.4	Aqueous electrophoresis of BSA/NGs-PEC (BSA/NGs 1:1) for determination of pI	108
Figure 4.5	Zeta potential of (A) BSA, (B) nanogels and (C) BSA/NGs-PEC (BF16) at pH 4.0	109
Figure 4.6	The standard calibration curve of BSA using Bradford reagent	110
Figure 4.7	Effect of BSA:NGs ratios (BF2 to BF7) on BSA/NGs PEC properties (A) particle size; (B) PdI; (C) zeta potential; (D) % EE and % DL at a fixed ratio 1:8, pH 4.0, incubation time 6 hour and stirring rate 100 rpm.	113
Figure 4.8	Effect of pH 1.2 (BF8), 4.0 (BF9) and 6.0 (BF10) on BSA/NGs PEC properties (A) particle size; (B) PdI; (C) zeta potential; (D) % EE and % DL at optimized BSA:NGs ratio 1:8, fixed incubation time 6 hour and stirring rate 100 rpm.	117
Figure 4.9	Effect of incubation time, 2 (BF11), 4 (BF12), 6 (BF13) and 8 hours (BF14) on BSA/NGs PEC properties (A) particle size; (B) PdI; (C) zeta potential; (D) % EE and % LE at optimized BSA/NGs ratio 1:8 and pH 4.0, and at fixed stirring rate 100 rpm	119
Figure 4.10	Effect of stirring rate, 0 (without stirring) (BF15), 100 rpm (BF16) and 200 rpm (BF17) on BSA/NGs PEC properties (A) particle size; (B) PdI; (C) zeta potential; (D) % EE and % DL at optimized BSA/NG ratio 1:8 and pH 4.0, and at fixed stirring rate 100 rpm.	121

Figure 4.11	<i>In vitro</i> release of BSA from BSA/NGs-PEC (BF16) in the SGF and SIF media	125
Figure 5.1	<i>In vitro</i> release of BSA from BF16-Tre2 after lyophilisation using 2% w/v trehalose in SGF and SIF	140
Figure 5.2	FTIR spectra of (A) pure BSA, (B) nanogels, (C) trehalose, (D) blank formulation (lyophilized nanogels without BSA), (E) BSA16-Tre2	142
Figure 5.3	SDS-PAGE results. Lane 1: unstained low range protein ladder; Lane 2: BSA standard; Lane 3: BSA released from lyophilized BF16-Tre2	144
Figure 5.4	<i>In vitro</i> release profile of BSA from BF16 liquid formulation stored at $5\pm3^{\circ}\text{C}$ in SGF.	151
Figure 5.5	<i>In vitro</i> release profile of BF16 liquid formulation stored at $5\pm3^{\circ}\text{C}$ in SIF	151
Figure 5.6	<i>In vitro</i> release profile of BF16 liquid formulation at $25\pm2^{\circ}\text{C}/75\pm15\%\text{RH}$ in SGF	153
Figure 5.7	<i>In vitro</i> release profile of BF16 liquid formulation at $25\pm2^{\circ}\text{C}/75\pm15\%\text{RH}$ in SIF	153
Figure 5.8	<i>In vitro</i> release profile of BF16-Tre2 lyophilized formulation stored at $5\pm3^{\circ}\text{C}$ in SGF	157
Figure 5.9	<i>In vitro</i> release profile of BF16-Tre2 lyophilized formulation stored at $5\pm3^{\circ}\text{C}$ in SIF	158
Figure 5.10	<i>In vitro</i> release profile of the BF16-Tre2 lyophilized formulation at $25\pm2^{\circ}\text{C}/75\pm15\%\text{RH}$ in SGF	159
Figure 5.11	<i>In vitro</i> release profile of the BF16-Tre2 lyophilized formulation at $25\pm2^{\circ}\text{C}/75\pm15\%\text{RH}$ in SIF	159
Figure 6.1	Representative chromatograms of (A) Buffer (ACN: Sodium Sulphate); (B) Novorapid (SIF); (C) Novorapid (SGF); (D) m-Cresol; (E) Nanogels; (F) Blank formulation	168
Figure 6.2	Standard calibration curve of insulin	172
Figure 7.1	Aqueous electrophoresis of insulin for determination of pI	190
Figure 7.2	Graphical illustration for the prediction of pH range of complex forming solution using the pI values of insulin and nanogels	191

Figure 7.3	Mechanism of PEC formation between negatively charged nanogels and positively charged insulin	193
Figure 7.4	Aqueous electrophoresis of Ins/NGs-PEC (Ins/NGs 1:1) for determination of pI	194
Figure 7.5	Zeta potential of (A) insulin, (B) nanogels and (C) Ins/NGs-PEC at pH 4.0	195
Figure 7.6	Effect of Ins:NGs ratios 1:20 (InF1), 1:30 (InF2), 1:40 (InF3) and 1:50 (InF4) on Ins/NGs-PEC properties (A) particle size; (B) PdI; (C) zeta potential; (D) % EE and % DL at a fixed pH 4.0, incubation time 6 hour and stirring rate 100 rpm	199
Figure 7.7	Effect of pHs 1.2 (InF5) 4.0 (InF6), 7.4 (InF7) on Ins/NGs PEC properties (A) particle size; (B) PdI; (C) zeta potential; (D) % EE and % DL at optimized Ins: NGs ratio 1:40, fixed incubation time 6 hour and stirring rate 100 rpm	203
Figure 7.8	Effect of incubation times 4 (InF8) , 6 (InF9) and 8 (InF10) hours on Ins/NGs-PEC properties (A) particle size; (B) PdI; (C) zeta potential; (D) % EE and % DL at optimized Ins/NG ratio 1:40 and pH 4.0, incubation time 6 hours and at stirring rate 100 rpm.	205
Figure 7.9	Effect of stirring rate 0 rpm (InF11), 100 rpm (InF12), 200 rpm (InF13) on the Ins/NGs PEC formulations properties (A) particle size; (B) PdI; (C) zeta potential; (D) % EE and % DL at optimized Ins/NG ratio 1:40, pH 4.0 and incubation time of 6 hours	208
Figure 7.10	<i>In vitro</i> release of insulin from Ins/NGs PEC (InF-12) in the SGF and SIF media	211
Figure 7.11	<i>In vitro</i> release of insulin from lyophilized Ins/NGs-PEC (InF12-Tre2) in SGF and SIF	214
Figure 7.12	FTIR spectra of (A) insulin (B) nanogels (C) trehalose (D) blank formulation lyophilized using trehalose (E) Ins/NGs-PEC (InF12-Tre2)	215
Figure 7.13	SDS-PAGE results. Lane 1: low range protein ladder; Lane 2: insulin released from formulation; Lane 3: Novorapid [®] Insulin	217
Figure 7.14	<i>In vitro</i> release profile of InF12 liquid formulation stored at 5±3°C in SGF	222
Figure 7.15	<i>In vitro</i> release profile of InF12 liquid formulation stored at 5±3°C in SIF	223

Figure 7.16	<i>In vitro</i> release profile of lnF12 liquid formulation stored at $25\pm 2^{\circ}\text{C}/75\pm 15\%\text{RH}$ in SGF	224
Figure 7.17	<i>In vitro</i> release profile of lnF12 liquid formulation stored at $25\pm 2^{\circ}\text{C}/75\pm 15\%\text{RH}$ in SIF	224
Figure 7.18	<i>In vitro</i> release profile of lnF12-Tre2 lyophilized formulation stored at $5\pm 3^{\circ}\text{C}$ in SGF	228
Figure 7.19	<i>In vitro</i> release profile of lnF12-Tre2 lyophilized formulation stored at $5\pm 3^{\circ}\text{C}$ in SIF	229
Figure 7.20	<i>In vitro</i> release profile of lnF12-Tres2 lyophilized formulation stored at $25\pm 2^{\circ}\text{C}/75\pm 15\%\text{RH}$ in SGF	230
Figure 7.21	<i>In vitro</i> release profile of lnF12-Tres2 lyophilized formulation stored at $25\pm 2^{\circ}\text{C}/75\pm 15\%\text{RH}$ in SIF	230
Figure 7.22	Effect of oral administration of the three doses (25, 50 and 100 IU/kg) of insulin loaded nanogels and four control groups on the percentage reductions in blood glucose level in the streptozotocin-induced diabetic rats	234
Figure 7.23	Comparison of serum concentration at T0 and T8 following oral administration of three doses (25, 50 and 100 IU/kg) of insulin loaded nanogels and four control groups.	237

LIST OF PLATES

		Page
Plate 2.1	Typical TEM micrograph of pH-sensitive MMA/IA nanogels dispersed in PBS pH 3.0 under different magnifications; (A) 10K (B) 20K. The scale bar meant 500nm	72
Plate 2.2	Typical TEM micrograph of MMA/IA nanogels dispersed in PBS pH 7.4 at magnification of 20K. Scale bar meant 200nm	75
Plate 3.1	Histo-pathological examination of major organs (heart, kidney, liver, spleen, brain, ovary, lungs, stomach, small intestine, large intestine) of female Sprague Dawley rats at 14 days after orally administered nanogels at the dose of 2000mg/kg body weight.	90
Plate 5.1	Physical appearance of lyophilized cake of BSA/NGs-PEC; (A) without cryoprotectant; (B) using 2%w/v mannitol (BF16-Mnt2); (C) 2% w/v trehalose (BF16-Tre2)	135
Plate 5.2	TEM A) BSA-loaded nanogels before lyophilization (BF16); B) BSA-loaded nanogels after lyophilization (BF16-Tre2) at magnification of 10K	145
Plate 5.3	SEM of reconstituted lyophilized BF16-Tre2 at different magnification; (A) 10K, (B) 30K	146
Plate 7.1	Physical appearance of insulin solution at different pH values	189
Plate 7.2	Transmission electron micrographs of reconstituted lyophilized InF12-Tre2 at magnification of 10K.	218

LIST OF ABBREVIATIONS AND SYMBOLS

°C	Degree centigrade
µg	Microgram
µl	Microliter
AA	Acrylic acid
AAm	Acrylamide
ALB	Albumin
ALP	Alkaline phosphatase
ALT	Alanine aminotransferase
ANOVA	Analysis of Variance
APS	Ammonium per-sulphate
AST	Aspartate aminotransferase
BPO	Benzoyl peroxide
BSA	Bovine serum albumin
BSA/NGs	Bovine serum albumin/Nanogels
BSA/NGs-PEC	BSA-nanogels polyelectrolyte complex
CD	Circular dichroism
CREA	Creatinine
DLS	Dynamic light scattering
DDS	Drug delivery system
EDTA	Diaminetetraacetic acid
EE	Entrapment efficiency
EGDMA	Ethylene glycol dimethacrylate
ELISA	Enzyme-linked immunosorbent assay

Fr	Refrigerator conditions (5±3°C)
FTIR	Fourier transform infrared spectroscopy
GLOB	Globulin
HDL	High-density lipoprotein
HEMA	2-hydroxyethyl methacrylate
HGB	Hemoglobin
HPC	Hydroxypropylcellulose
HPLC	High performance liquid chromatography
HPMA	2- hydroxypropyl methacrylate
HPMC	Hydroxyl-propylmethylcellulose
HPMC/PAA	Hydroxypropylmethylcellulose/poly- (acrylic acid)
Ins	Insulin
IA	Itaconic acid
IDDM	Insulin-dependent diabetes mellitus
IDF	International Diabetes Federation
LbL	Layer-by-layer
LCST	Lower critical solution temperature
LDL	Low-density lipoproteins
LE	Loading efficiency
Liq	Liquid formulation
LOD	Limit of detection
LOQ	Limit of quantification
Lyo	Lyophilization
MAA	Methacrylic acid
MBAAm	<i>N,N</i> -methylenebisacrylamide

MCH	Mean corpuscular hemoglobin
MCHC	Mean corpuscular hemoglobin concentration
MCV	Mean corpuscular volume
mg	Milligram
min	Minute
ml	Milliter
MMA	Methyl methacrylate
MTT	3-[4,5-dimethylthiazol-2-yl]-2, 5-diphenyl tetrazolium bromide
Mw	Molecular weight
MWCO	Molecular weight cut off
Nanogels	NGs
N	Theoretical plate number
NIDDM	Noninsulin-dependent diabetes mellitus
NIPAAm	<i>N</i> -isopropyl acrylamide
NIPAAm–MAA–HEMA	N-Iso propyl acryl amide-methacrylic acid-hydroxy ethyl methacrylate
nm	Nano-meter
NMR	Nuclear magnetic resonance
Opt	Optimization
OEOMA	Oligo(ethylene glycol) monomethyl ether methacrylate
PCP	Poly(methacrylic acid–chitosan–polyethylene glycol)
PCV	Packed cell volume
PEC	Polyelectrolyte complex
PEG	Poly ethylene glycol

PEGDA	Poly(ethylene glycol) diacrylate
PEGDMA	Poly(ethylene glycol) dimethacrylate
pI	Isoelectric point
PLGA	Poly (lactic-co-glycolic acid)
PLT	Platelet
PMAA	Poly (methacrylic acid)
PNIPAAm-co-AAc	Poly (N-isopropylacrylamide-co-acrylic acid)
PNIPAAm-co-NVA	(N-isopropylacrylamide)-co-N-vinylacetamide
PNIPAM	N-isopropylacrylamide
PNIPAM-PAA	Poly N-isopropylacrylamide-poly acrylic acid
PPs	Peyer's patches
PVA	Poly (vinyl alcohol)
RBC	Red blood cells
RDW	RBC distribution width
RE	Relative error
RH	Relative humidity
Ro	Room conditions (25±2°C/75±15%RH)
rpm	Rotation per minute
RSD	Relative standard deviation
SEM	Scanning electron microscope
SGF	Simulated gastric fluid
SIF	Simulated intestinal fluid
STZ	Streptozotocin
T0M	Time zero months (immediately after preparation)
T1M	Time one month

T2M	Time two months
T3M	Time three months
T6M	Time six months
TBIL	Total bilirubin
TEER	Trans-epithelial electrical resistance
TEM	Transmission electron microscopy
TF	Oligothiophene fluorophore
TJ	Tight junctions
TP	Total protein
USP	United States Pharmacopoeia
UV	Ultraviolet
WCC/WBC	White cell count/white blood cells

SINTESIS DAN PENCIRIAN NANOGEL POLIELEKTROLIT SENSITIF-pH UNTUK PENGHANTARAN ORAL BAGI ALBUMIN SERUM BOVIN DAN INSULIN SEBAGAI PROTEIN MODEL

ABSTRAK

Peptida dan protein diberikan secara parenteral kerana ketidakstabilan dan ketidakstabilan bio melalui laluan oral. Pentadbiran parenteral dikaitkan dengan pematuhan pesakit miskin akibat kesakitan dan ketidakselesaian melalui pelbagai suntikan. Pentadbiran oral boleh memberi manfaat untuk meningkatkan pematuhan pesakit dan tindak balas fisiologi terhadap peptida dan protein (contohnya insulin). Tujuan kajian ini adalah untuk mensistesis nanogel polielektrolit MMA/IA sensitif pH untuk digunakan sebagai pembawa untuk penghantaran oral protein model (Albumin Serum Bovin dan insulin). Nanogel disintesis menggunakan monomer metil metakrilat (MMA), asid itakonik (IA) dan pautan silang etilena glikol dimetacrilat (EGDMA) melalui proses pempolimeran radikal bebas. Beberapa parameter dioptimumkan semasa sintesis nanogel MMA/IA sensitif pH. Parameter optimum untuk sintesis nanogel ialah etanol/air 70/30 v/v, isipadu pencairan 96/57.6 v/v, EGDMA 1.5 mol % dan MMA/IA 70/30 mol %. Spektrum ^1H NMR dan FTIR memperlihatkan ketiadaan puncak proton vinil MMA, IA dan EGDMA, menunjukkan sintesis nanogel telah berjaya. LC-TOF-MS menunjukkan berat molekul 934.717. Analisis XRD memperlihatkan nanogel dalam bentuk amorfus dan nisbah pengembangannya 8.08 ± 0.64 pada pH 7.4. Saiz zarah nanogel 229.10 ± 2.09 nm, indeks polisebaran (PDI) 0.111 ± 0.03 dan potensi zeta -43.1 ± 1.81 mv. Analisis mikroskop transmisi elektron (TEM) memperlihatkan bahawa nanogel mempunyai bentuk yang tidak teratur. Ketoksikan *in vitro* dengan ujian MTT menggunakan sel Caco-2 menunjukkan bahawa nanogel adalah tidak toksik pada kepekatan 0.25, 0.5

dan 1 mg/ml. Manakala, kajian toksisiti *in vivo* menggunakan tikus Sprague Dawley juga menunjukkan bahawa nanogel pada dos 2000 mg/kg berat badan tidak toksik. Formulasi cecair terpilih BSA/NGs-PEC (BF16) dan Ins/NGs-PEC (InF12) menunjukkan nisbah kompleksasi optimum antara BSA:nanogel 1:8 dan insulin:nanogel 1:40. Formulasi BF16 mempunyai saiz zarah 287.87 ± 8.86 nm dan kecekapan pemerangkapan (% EE) sebanyak 89.32 ± 4.36 %. Sementara itu, formulasi BF16 dibeku-kering menggunakan trehalos (BF16-Tre2) mempunyai saiz zarah 324.10 ± 16.75 nm dan % EE 85.44 ± 2.19 %. Formulasi InF12 mempunyai saiz zarah 190.43 ± 0.90 nm dan % EE sebanyak 85.18 ± 2.33 %. Manakala formulasi InF12 yang dibeku-kering menggunakan trehalose (InF12-Tre2) mempunyai saiz zarah 430.50 ± 27.61 nm dan % EE 82.15 ± 2.12 %. BSA dibebaskan dari formulasi BF16 sebanyak 7.65 ± 1.82 % dalam SGF dan 92.17 ± 2.23 % dalam SIF. Sementara itu pembebasan BSA dari formulasi BF16-Tre2 13.21 ± 4.0 % dalam SGF dan 95.16 ± 4.16 % dalam SIF. Pembebasan insulin dari InF12 adalah 33.53 ± 4.01 % dalam SGF dan 91.43 ± 4.50 % dalam SIF. Manakala pembebasan insulin dari InF12-Tre2 adalah 28.71 ± 3.81 % dalam SGF dan 96.53 ± 5.09 % dalam SIF. Data kajian kestabilan menunjukkan bahawa formulasi BF-16Tre2 dan InF12-Tre-2 stabil dalam penyimpanan 5 ± 3 °C selama kajian kestabilan. Ujian SDS-PAGE memperlihatkan bahawa struktur utama BSA dalam formulasi BF16-Tre2 dan insulin dalam formulasi InF12-Tre2 tidak berubah. Kajian *in vivo* pada tikus diabetes berikutan pemberian oral formulasi InF12-Tre2 yang mengandungi dos insulin 100 IU/kg berat badan telah menurunkan kadar glukosa dengan signifikan kepada 51.1 ± 5.5 % selepas 6 jam dan peningkatan konsentrasi insulin serum setelah 8 jam. Sebagai kesimpulan, nanogel adalah pembawa harapan bagi penghantaran protein secara

oral, dan formulasi InF12-Tre2 mungkin berpotensi untuk penghantaran insulin secara oral.

**SYNTHESIS AND CHARACTERIZATION OF pH-SENSITIVE
POLYELECTROLYTE NANOGELS FOR ORAL DELIVERY OF BOVINE
SERUM ALBUMIN AND INSULIN AS MODEL PROTEINS**

ABSTRACT

Peptide and protein are administered parentally owing to their instability and insufficient bioavailability through oral route. Parenteral administration is associated with poor patient compliance due to pain and discomfort by multiple injections. Oral administration can be beneficial to improve patient compliance and physiologic response to peptide and protein (e.g. insulin). The aim of the present study was to synthesize pH sensitive polyelectrolyte methyl methacrylate/itaconic acid (MMA/IA) nanogels to be used as a carrier for oral delivery of model proteins (BSA and insulin). The nanogels were synthesized using monomers methyl methacrylate (MMA), itaconic acid (IA) and a crosslinker ethylene glycol dimethacrylate (EGDMA) via free radical polymerization. Several parameters were optimized during the synthesis of pH sensitive MMA/IA nanogels. The optimized parameters to synthesis the nanogels were ethanol/water 70/30 v/v, dilution volume 96/57.6 v/v, EGDMA 1.5 mol % and MMA/IA 70/30 mol %. The ^1H NMR and FTIR spectra showed absence of vinyl proton peaks of MMA, IA and EGDMA, thus indicating successful synthesis of nanogels. The LC-TOF-MS showed that the molecular weight was 934.717. The XRD analysis revealed that the nanogels were in the amorphous form and had the swelling ratio of 8.08 ± 0.64 at pH 7.4. The nanogels had the particle size of 229.10 ± 2.09 nm, polydispersity index (PDI) of 0.111 ± 0.03 and zeta potential of -43.1 ± 1.81 mv. The transmission electron microscope (TEM) analysis showed that the nanogels had irregular shape. The *in vitro* toxicity performed by MTT assays using caco-2 cell revealed that the nanogels

was nontoxic at concentrations of 0.25, 0.5 and 1 mg/ml. Meanwhile, the *in vivo* toxicity study using Sprague Dawley rats also showed that the nanogels at a dose of 2000 mg/kg body weight was non-toxic. The selected BSA/NGs-PEC (BF16) and Ins/NGs-PEC (InF12) liquid formulations showed the optimum complexation ratio between BSA:nanogels at 1:8 and insulin:nanogels at 1:40. The BF16 formulation had the particle size of 287.87 ± 8.86 nm and % entrapment efficiency (%EE) of 89.32 ± 4.36 %. Meanwhile, the lyophilized BF16 formulation using trehalose (BF16-Tre2) had the particle size of 324.10 ± 16.75 nm and % EE of 85.44 ± 2.19 %. The InF12 formulation had the particle size of 190.43 ± 0.90 nm and % EE of 85.18 ± 2.33 %. While, the lyophilized InF12 formulation using trehalose (InF12-Tre2) had the particle size of 430.50 ± 27.61 nm and % EE of 82.15 ± 2.12 %. The release of BSA from BF16 formulation was 7.65 ± 1.82 % in SGF and 92.17 ± 2.23 % in SIF. Meanwhile, the release of BSA from BF16-Tre2 formulation was 13.21 ± 4.0 % in SGF and 95.16 ± 4.16 % in SIF. The release of insulin from InF12 was 33.53 ± 4.01 % in SGF and 91.43 ± 4.50 % in SIF. Meanwhile, the release of insulin from InF12-Tre2 was 28.71 ± 3.81 % in SGF and 96.53 ± 5.09 % in SIF. The stability study data revealed that the BF-16Tre2 and InF12-Tre-2 formulations stored at 5 ± 3 °C were stable during the stability study period. The SDS-PAGE assay indicated that the primary structure of BSA in the BF16-Tre2 and insulin in the InF12-Tre2 formulations were intact. The *in vivo* study in the diabetic rats following oral administration of 100 IU/kg body weight InF12-Tre2 formulation had reduced blood glucose level significantly to 51.1 ± 5.5 % after 6 hours and increased serum insulin concentration significantly after 8 hours. In conclusion, the nanogels are promising carriers for oral delivery of proteins, and InF12-Tre2 formulation may have potential for oral delivery of insulin.

CHAPTER 1

INTRODUCTION

1.1 Peptide and protein therapeutics

Peptides and proteins are building units of life and are now gaining considerable attention as therapeutic groups. The current market for peptide and protein drugs is estimated to be greater than 4 billion USD per year (Craik et al., 2013). The global peptides drug market has been predicted to increase from US\$ 14.1 billion in 2011 to an estimated US\$ 25.4 billion in 2018 (Fosgerau and Hoffmann, 2015). As compared to small molecular drugs the market of peptide and protein drugs is growing very fast and is expected to attain much larger proportion of market in the near future (Craik et al., 2013). The peptide based medicine Lupron from Abbott Laboratories achieved global sale of more than US\$ 2.3 billion in 2011, while Lantus from Sanofi reached sale of US\$ 7.9 billion in 2013 (Kaspar and Reichert, 2013).

The understanding of molecular biology of macromolecular endogenous proteins, and their role in various pathological conditions has resulted in realization of therapeutic potential of peptide and protein. The therapeutic role of peptide and protein in different ailments like diabetes, cancer and genetic diseases has drastically increased their recognition as drug. The advantages of using peptide and protein as therapeutics are because of the following reasons; (i) proteins are highly specific in their response, (ii) show less interference with normal biological processes and have reduced side effects, (iii) well tolerate-ability and less likely to evoke immune response and (iv) effective alternative for treatment without need for gene therapy (because for diseases caused by gene mutation or deletion, protein drugs are effective in treatment without requiring gene therapy) (Leader et al., 2008).

Additionally, the problem of availability of peptide and protein drugs at commercial scale has been overcome to a certain extent due to extensive research in the field of recombinant DNA, peptide and protein engineering and tissue culture techniques. However, their formulation and optimum delivery is still considered as a substantial challenge to pharmaceutical scientists. To date, peptide and protein based therapies that have been unsuccessful are more numerous than the successful ones. This is because huge number of challenges or issues needs to be resolved in developing successful peptide and protein loaded formulations.

1.1.1 Current routes of peptide and protein administrations and limitations

The low bioavailability of peptide and protein drugs after administration by the oral or non-oral mucosal route is due to poor permeability characteristics involving brush border, luminal, cytosolic metabolism, and hepatic clearance mechanisms (Aungst, 1993). Hence, at present approximately 75% of peptide and protein drugs are administered parentally. Among these, intravenous (i.v.) and subcutaneous delivery are the most popular methods for administrations of peptide and protein therapeutics (Langer et al., 1985). This route has solved the problem of bioavailability by enhancing the absorption of high molecular weight peptide and protein drugs. However, frequent injections, oscillating plasma drug profiles and low patient acceptability make parenteral administration problematic.

Additionally, parenteral administration has revealed the emergence of numerous shortcomings in addition to the bioavailability issue, such as non-covalent complexation with blood products, dissociation of protein subunit, conformational changes, destruction of labile side groups, opsonization and rapid metabolism (Fosgerau and Hoffmann, 2015, Torchilin, 2008). These shortcomings have

prompted researchers to develop effective delivery system to deliver therapeutic peptide and protein with ease and efficiency.

1.2 Challenges in oral peptide and protein delivery

1.2.1 Critical issues with physicochemical properties of peptide and protein

An undesirable physicochemical characteristic, low bioavailability, lack of effective route and method of delivery has resulted in only limited use of peptide and protein as therapeutic agents. Various critical issues associated with peptide and protein therapeutics include (i) difficult to cross absorption barriers due to high molecular weight and possessing both hydrophilic and hydrophobic units, (ii) high susceptibility to various physical and chemical environmental conditions due to tertiary structure, (iii) short *in-vivo* biological half-life due to rapid clearance through liver and (iv) potent nature that requires precise dosing (Humphrey and Ringrose, 1986).

1.2.2 *In vivo* barriers associated with oral peptide and protein delivery

Before pharmaceutical macromolecular therapeutic peptide and protein reach their final destination, they have to face a number of challenges or barriers. An overview of three major *in vivo* barriers in oral peptide and protein delivery is presented in Figure 1.1 (Mudassir et al., 2015). These include; (i) the acidic environment of the stomach, (ii) intestinal enzymes and (iii) intestinal epithelium tight junctions (Khafagy et al., 2007).

The efficiency of orally administered peptide and protein is hindered by chemical, physical and enzymatic environment of GIT (Humphrey and Ringrose, 1986). As soon as these drugs are administered, their stability is affected by highly acidic conditions of the stomach. The major classes of proteases (e.g. serine, cysteine,

threonine, aspartic and metallo- proteinases, trypsin, carboxypeptidase and chymotrypsin) are secreted mostly in the duodenum (Lee et al., 1991). These proteases are responsible for 20% enzymatic degradation of orally administered peptide and protein. Moreover, large amount of peptidases on the brush border of epithelial cells as well as in the lumen of the small intestine are also responsible for *iv-vivo* degradation of peptide and protein (Allémann et al., 1998). Additionally, mucous turnover, and peristalsis movements further reduces the chances of peptide and protein to come in contact with and cross epithelial barrier.

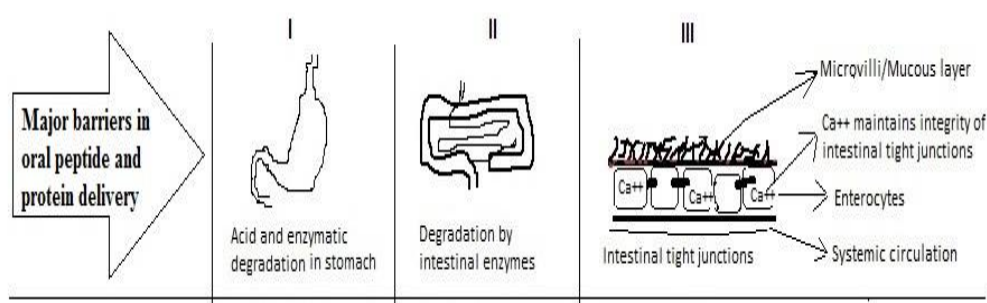


Figure 1.1: An overview of three major *in vivo* barriers in oral peptide and protein delivery (Mudassir et al., 2015)

For the peptide and protein drugs that gained access to the surface of the epithelium, their diffusion is further hindered by mucous, villi, microvilli and brush border glycol-calyx (a layer of sulphated muco-polysaccharides) (Sanderson et al., 1994). These barriers are of significance because peptide and protein drugs are transported across epithelium cells in order to gain access to blood circulation. The mucosal layer contains glycol-calyx which is located apical to the epithelial cell barrier. The mucosal layer is additionally composed of mucins which are heavily glycosylated high molecular weight proteins. An unstirred layer is created near the epithelial surface which is due to limited bulk flow to epithelial cells (Aoki et al., 2005). An

overview of the intestinal barriers to peptide and protein delivery is presented in Figure 1.2.

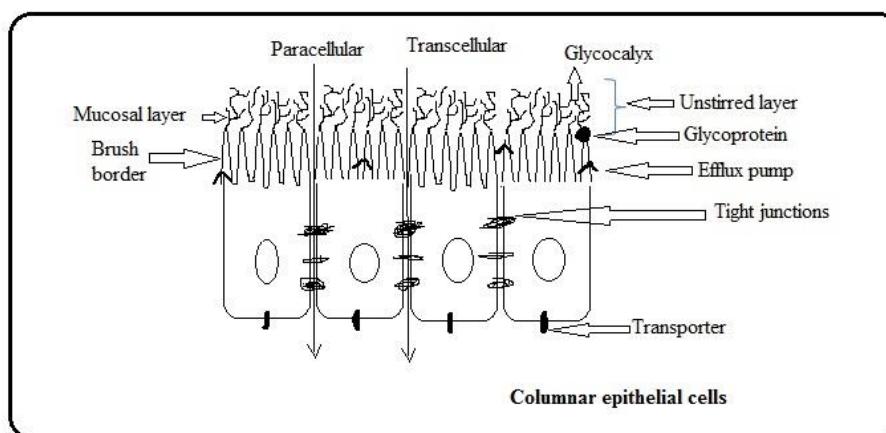


Figure 1.2: Intestinal barriers to peptide and protein delivery (the intestinal epithelial barriers is composed of single layer of columnar epithelial cells and mucosal layer present on the apical side) (Chen et al., 2011).

1.3 Transportation of peptide and protein and loaded nanocarriers across the intestinal epithelium

The transport mechanisms of peptide and protein across the intestinal epithelium may involve (i) trans-cellular pathways (ii) para-cellular pathways and (iii) specific uptake of ligand-modified nanocarriers. An overview of transport mechanisms of peptide and protein drugs delivered by nanocarriers across the intestinal epithelium is presented in Figure 1.3A and B.

1.3.1 Trans-cellular pathways

The transportation of peptide and protein loaded nanocarriers via trans-cellular pathways involves the passage of nanocarriers through enterocytes or M cells of Peyer's patches (Roger et al., 2010, Shakweh et al., 2004). Apparently, the high molecular weight peptide and protein loaded nanocarriers cannot diffuse through cells by passive diffusion due to large size. In contrast, different energy-dependent mechanisms (active transport) could facilitate the transport of peptide and protein

loaded nanocarriers. The active trans-cellular transport of nanocarriers is initiated in the endocytosis at the apical cell membrane and transported across the cell. Finally, the nanocarriers are released in baso-lateral pole (Burton et al., 1991). The trans-cellular pathways generally depend upon the particle size, surface charge and muco-adhesion characteristic of nanocarriers (Roger et al., 2010, Shakweh et al., 2005, Shakweh et al., 2004). It has been demonstrated that particle size between 50 to 500 nm had shown optimum interaction between nanocarriers and epithelial cells (Desai et al., 1996). Shakweh et al. (2005) reported the effect of surface charge on non-specific uptake by enterocytes or M cells. They found the negatively charged nanoparticles had better uptake by Peyer's patches. Additionally, the uptake by epithelial cell was also enhanced for materials showing muco-adhesion. The muco-adhesion increased residence time as well as contact of peptide and protein loaded nanocarriers over epithelium thus increasing drug concentration at absorption site. The hydrophilic polymers such as poly acrylic acid (PAA), thiomers and chitosan (CS) and their derivatives also showed the muco-adhesive properties (Takeuchi et al., 2001).

1.3.2 Para-cellular pathway

The para-cellular pathway is considered as the preferred route for transporting high molecular weight peptide and protein drugs. Para-cellular space occupies less than 1% of total mucosal surface. Practically, the passage of peptide and protein loaded nanocarriers approximately larger than 1 nm is completely hindered by intestinal tight junctions (Nellans, 1991). Therefore, it is well recognized that the para-cellular route does not allow the passage of nanocarriers or peptide and protein. However, the success of para-cellular transportation relies upon the reversible opening of intestinal tight junctions (TJs) (Nellans, 1991). Fortunately, certain polymers have

shown capability to reversibly open TJs. Among these, the anionic polymers (such as poly acrylic acid), cationic polymers (such as chitosan and its derivatives) and calcium chelators are the most prominent examples. Poly acrylic acid (PAA) and chitosan (CS) generally act by interacting with surface receptors or extracellular domains of TJ proteins. Thus, activating cascade that results in opening of TJs. The calcium chelating TJs are opened via activation of protein kinase C (Salamat-Miller and Johnston, 2005).

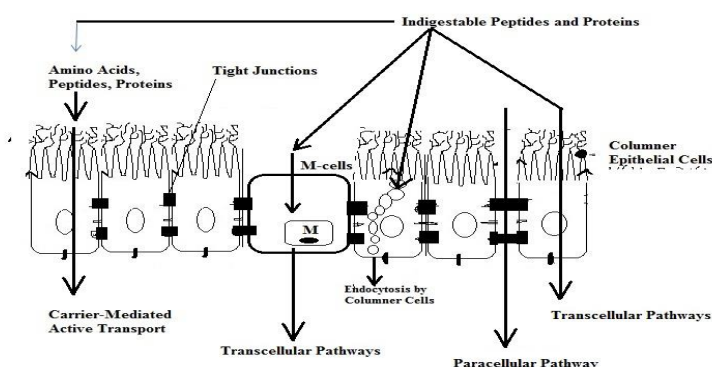
1.3.3 Specific uptake of ligand-modified nanocarriers

In order to increase cellular uptake, nanocarriers are modified by covalently conjugating or adsorbing ligands (e.g. vitamins or other proteins) to their surface. For example, lectins (a class of protein that can bind to cell membrane) were conjugated to the nanoparticles, which resulted in an increase in the protein transport across intestinal mucosa, especially through Peyer's patches and M cells (Hussain et al., 1997). The authors investigated the intestinal uptake of orally administered inert nanoparticles where their surface was conjugated with tomato lectin. It was observed that lectin-conjugated nanoparticles showed 15 times increase in intestinal uptake. Another approach to increase oral uptake of various peptide and protein therapeutics is the use of vitamin B12. The Vitamin B12 formed complex with intrinsic factor (IF) present in the small intestine. The vitamin B12-IF complex was identified by IF-specific receptor present on the luminal surface of intestinal cells, which aids in transporting across intestinal enterocytes (Russell-Jones, 1998).

Although the specific uptake of ligand-modified nanocarriers (for example specific-receptor-mediated trans-cytosis) has shown encouraging outcomes, the major limitations were (i) inadequate absorption of peptide and protein loaded nanocarriers

(ii) adequate amount of ligand must be bound to the particle surface for achieving optimum therapeutic effect (iii) toxicity as well as possible immune response arising due to continuous absorption of particles by M cells into Peyer's patches (Khafagy et al., 2007).

(A)



(B)

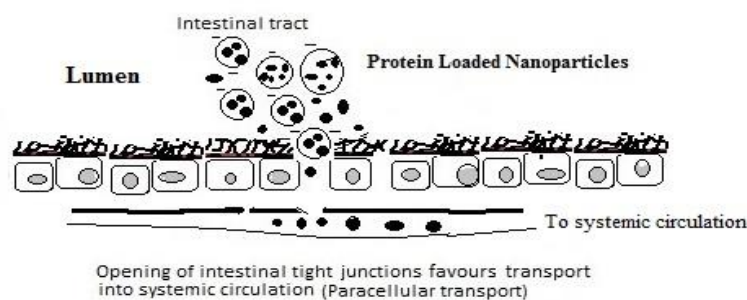


Figure 1.3: Transport mechanisms; (A) uptake of peptide and protein drugs across the intestinal epithelium; (B) translocation of protein loaded nanoparticles through paracellular pathway (Mudassir et al., 2015, Chen et al., 2011)

1.4 Approaches to overcome oral peptide and protein delivery barriers

The primary objective of oral peptide and protein delivery is to protect loaded peptide and protein from stomach acid, luminal proteases and to facilitate their transport across the intestinal epithelium. To overcome these absorption barriers,

various approaches/ technologies have been used. These approaches are discussed as follows:

1.4.1 Enteric coating

Enteric coating has been used traditionally to protect peptide and protein from the acidic environment of the stomach. However, the efficiency and reliability of enteric coating was limited due to variable pH and enzymes present in the GI tract. Additionally, the enteric polymers are subjected to uncontrolled polymerization during storage and handling, thus resulting in poor control of the release of macro-molecules at the target site (Hussan et al., 2012). Therefore, there is a need to develop advanced pharmaceutical technologies to protect peptide and protein from enzymatic and intestinal absorption barriers.

1.4.2 Permeation or absorption enhancers

It is known that co-administration of peptide and protein with permeation enhancers significantly improved absorption (Lee, 1990). Generally, permeation enhancers act by combination of several mechanisms such as (i) by increasing para-cellular transport of peptide and protein through disruption and opening of tight junctions (TJs), (ii) reducing mucous viscosity and (iii) increasing membrane fluidity. The major classes of permeation enhancers include surfactants (sodium lauryl sulfate, poly-sorbitate and tween 80), bile salts (sodium glycholate and sodium deoxycholate) and fatty acids (sodium caprate, acyl carnites, oleic acid and lauric acid) (Fasano and Uzzau, 1997, Mesiha et al., 1994). Surfactants act by disrupting intestinal membrane, and cause an increase in membrane permeability of peptide and protein across the cell epithelium (trans-cellular pathway) (Xia and Onyuksel, 2000). Bile salts decreases mucus viscosity and peptidase activity, while promoting disruption of phospholipid acyl chain and formation of mixed micelles (Sakai et al.,

1997). Similarly, fatty acids act through modulating para-cellular permeability (Anilkumar et al., 2011). The efficiency of permeation enhancers is influenced by the nature of peptide and protein, the nature of permeation enhancers and capability of delivery system to release permeation enhancers (Nishihata et al., 1984). The major drawback of this approach is the potential toxicity of permeation enhancers on intestinal epithelial cells. The disruption of intestinal tight junctions through continuous and irreversible opening of tight junctions may increase transport of toxins and other biological pathogens (Swenson et al., 1994). Nevertheless the use of permeation enhancers is considered as an effective approach for oral peptide and protein delivery, however the toxicity issues related to the excipients has to be addressed, especially when it is used in the treatment of chronic disease.

1.4.3 Enzyme inhibitors

Enzyme inhibitors prevent inactivation of peptide and protein drugs by digestive enzymes. For this purpose, both enzyme inhibitors and peptide and protein therapeutics are co-administered to increase oral bioavailability. Enzyme inhibitors act by binding reversibly/irreversibly to the target enzyme, thus resulting in inactivation and reduced enzymatic activity (Copeland, 2013). Various drugs used as enzyme inhibitors include sodium glycocholate, bacitracin, puromycin, camostat mesilate, chicken ovomucoid (trypsin inhibitor), aprotinin (inhibitor of trypsin and chymotrypsin), soybean trypsin inhibitor (inhibitor of pancreatic endopeptidases) (Bernkop-Schnürch, 1998, Yamamoto et al., 1994). The major drawback of this approach is the potential toxic effect due to the enzyme inhibitors themselves. Moreover, the enzyme inhibitors may result in excessive reduction in normal enzymatic activity *in vivo* and disrupt normal absorption of dietary peptide and protein (Knarreborg et al., 2003, Bernkop-Schnürch, 1998). An alternate approach to

observe enzyme inhibition is to alter pH at the site of action because the stomach enzymes are effective only at acidic pH (approximately 2) (Piper and Fenton, 1965).

1.4.4 Physicochemical modification of peptide and protein

The physicochemical modification of peptide and protein involve conjugation with polymers to improve membrane permeability and proteolytic stability (Herman et al., 1995). The immune response induced by peptide and protein can be modified through chemical modifications. Various approaches for physicochemical modification of peptide and protein include (i) protein-polymer conjugation, (ii) pegylation (iii) amino acid alterations and (iv) hydrophobizations.

The protein-polymer conjugations require polymers which should be non-immunogenic, water soluble, biocompatible and biologically inert. Generally, polymers used for peptide and protein conjugations must be capable to augment the intrinsic properties of bio-macromolecules, while they should not diminish biological activity or boost toxicity. *N*-(2-hydroxypropyl) methylacrylamide and poly (ethylene glycol) are the most widely used polymers for peptide and protein conjugation (Carter et al., 2016, Grover and Maynard, 2010, Naipu et al., 2010).

Pegylation is the process where poly(ethylene glycol) (PEG) is covalently attached to peptide and protein which result in improvement of therapeutic potential (D'souza and Shegokar, 2016). The advantage of pegylation is the formation of steric shield which protects the peptide and protein from recognition by macrophages (body's immune response). It also enhances stability of peptide and protein against enzymes. Additionally, the increase in particles size also reduces renal clearance (D'souza and Shegokar, 2016).

The enzymatic stability of peptide and protein can also be achieved through chemical modifications. The modifications involve the replacement of one or more L-amino acids with D-amino acids which are responsible for enzymatic cleavage (Tugyi et al., 2005). The development of various analogs of the endogenous opioid penta-peptide methionine (Met)-enkephalin is the example of chemical modification (Bohner et al., 1994).

The surface modifications of peptide and protein are achieved through hydrophobization process in which hydrophobic unit added within the peptide and protein backbone (Yuan et al., 2011). For example the covalent conjugation of fatty acids with insulin and desmopressin significantly increased intestinal permeability (Kahns et al., 1993, Hashizume et al., 1992). Although the physicochemical modifications showed valuable improvement in transport of peptide and protein, however, these methodologies increased the risk of declining therapeutic and biological activity of peptide and protein.

1.4.5 Muco-adhesive polymeric systems

Mucoadesive polymeric systems act by prolonging the gastrointestinal residence time. They protect the drug from the harsh environment of the stomach and enhance absorption of loaded peptide and protein across the intestinal epithelium (Khan et al., 2013, Rekha and Sharma, 2013, Rekha and Sharma, 2009, Rekha and Sharma, 2008a, Rekha and Sharma, 2008b). Thiolated polymers are popular examples of muco-adhesive systems. However, some drawbacks have been observed regarding *in vivo* performance of mucoadesive polymeric systems, such as prevention of free movements (Hwang et al., 1998, Claesson et al., 1995, Perez and Proust, 1987).

1.4.6 Alternative approaches for enhancing the absorption of peptide and protein

The alternative approaches include the use of eutectic mixtures and cell-penetrating peptides (CPPs). These approaches help in improving the solubility and permeability, thus facilitating the transport of peptide and protein across the cellular membranes. The use of eutectics in polymeric delivery system has not yet been extensively explored (Tuntarawongsa and Phaechamud, 2012). Recently the use of borneol/menthol eutectic mixture has been reported to enhance bioavailability of polypeptide (daidzein) in the treatment of breast and colon cancer (Shen et al., 2011). However, borneol/ menthol eutectic mixture had toxic effect towards tight junctions (Tscheik et al., 2013). The cell-penetrating peptides (CPPs) act by enhancing permeability through the intestinal epithelial cells (Foged and Nielsen, 2008). The positive effects of CPPs on the intestinal absorption of peptide and protein have been observed. It was demonstrated that high dose of CPPs was required to achieve the desired therapeutic effect of peptide and protein drugs (Morishita et al., 2007). However, multiple administrations of CPPs doses may cause toxic effect. Therefore, it was concluded that safer and effective CPPs are required for oral delivery of peptide and protein (Morishita et al., 2007).

1.5 Characteristics of ideal oral peptide and protein delivery systems

Researchers in the field of pharmaceutical technology have been searching for efficient and effective nanocarriers which could be used to overcome oral peptide and protein delivery challenges. To date there are several peptide and protein delivery systems available which have been widely explored. Among these delivery systems only a few can fulfil most of the requirements of ideal drug delivery

systems (DDS). The characteristics of ideal DDS are presented in Figure 1.4 (Mudassir et al., 2015).

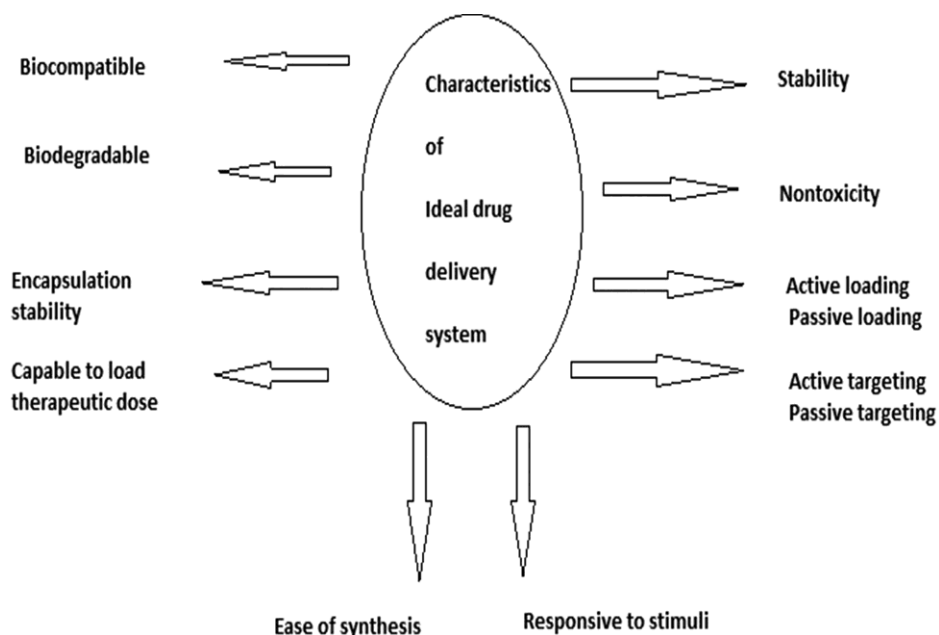


Figure 1.4: Characteristics of ideal DDS (Mudassir et al., 2015)

1.6 Oral peptide and protein delivery systems

1.6.1 Micro or nano-emulsions

Micro and nano-emulsions have shown capability to protect loaded peptide and protein from chemical and enzymatic degradation when administered through the oral route. They are generally classified into three categories such as (i) oil-in-water (o/w), (ii) water-in-oil (w/o), and (iii) bi-continuous micro-emulsions. They are promising in improving the bioavailability of hydrophobic molecules, including hydrophobic peptides, for example cyclosporine A (Ritschel, 1996, Sarciaux et al., 1995). Sun et al. (2012) developed novel nano-emulsion DDS using BSA as model protein to improve its stability. The BSA nano-emulsion showed average particle diameter of about 21.8 nm and encapsulation efficiency (>90%). The loaded BSA showed good structural integrity and specificity for the primary, secondary, and

tertiary structures, and also good bioactivity. Generally, the biggest challenge in utilizing micro or nano-emulsion in peptide and protein delivery was to overcome its low loading capacity and low physicochemical stability during storage.

1.6.2 Liposomes

Liposomes are lipid based delivery systems and have been extensively used for delivery of peptide and protein drugs. Kowapradit et al. (2012) prepared BSA-loaded *N*-(4-*N,N*-dimethylaminobenzyl) chitosan coated liposomes (TM₅₆Bz₄₂CS-coated LP-BSA) for oral protein drug delivery. The mean particle size and zeta-potential of the TM₅₆Bz₄₂CS-coated LP-BSA were 128 ± 15 nm and 5.38 ± 1.66 mV, respectively. The results revealed that the transport of FITC-BSA from TM₅₆Bz₄₂CS-coated FITC-BSA-LP was enhanced due to increased protein permeability across the Caco-2 cell monolayers. These liposomes were nontoxic and showed protection for loaded protein against degradation. Although some promising results were obtained using liposomes as peptide and protein carriers, however, the use of conventional liposomes is still limited. After extensive research for many years, it turned out that it was extremely challenging to overcome certain vital physicochemical and biological properties of liposomes e.g. leakage of drug molecules and short residence time in blood. Thus, due to these obstacles the use of liposomes for peptide and protein delivery is limited (Lasic, 1998).

1.6.3 Chitosan based nanoparticles

Chitosan (CS) is a polysaccharide obtained by deacetylation of chitin. Chitin is a hard substance that occurs widely in nature, particularly in the exoskeletons of arthropods such as crabs, prawns, insects and spiders. The building blocks of CS are glucosamine and N-acetyl-glucosamine (Thanou et al., 2001). CS is a suitable

carrier for delivery of peptide and protein to the small intestine due to their excellent muco-adhesive characteristics. The mechanism of muco-adhesion involves the interaction between the negatively charged sialic-acid groups in mucin and the positively charged CS (Bravo-Osuna et al., 2007). Additionally, CS was reported as a promising carrier for oral peptide and protein delivery owing to its capability to reversibly open intestinal tight junctions (TJs). Yeh et al. (2011) investigated the mechanism of TJs opening in Caco-2 cells treated with CS. The results revealed that para-cellular permeability (TJs opening) was due to redistribution of claudin-4 (CLDN4) from the cell membrane to the cytosol, which was associated with its degradation in lysosomes. Consequently, the TJ strength was diminished. It was further reported that the recovery of TJs depends on CLDN4 synthesis. It was suggested that multiple mechanism could be involved during opening of TJs. However, the usage of CS for oral peptide and protein delivery is limited due to it being insoluble at neutral/basic pH (Smith et al., 2004).

1.6.4 Poly (lactide-co-glycolide) (PLGA) nanoparticles

Nanoparticles consisting of PLGA have been widely investigated due to their biodegradability and biocompatibility. The hydrophobic nature of PLGA generally makes them unsuitable for entrapping water soluble peptide and protein drugs. Cheng et al. (2006) developed magnetically responsive polymeric poly(lactide-co-glycolide) (PLGA) microparticles for oral delivery of protein drugs. The protein drug (insulin) was encapsulated in the PLGA microparticles. Hypoglycemic effect was evaluated in mice in the presence of applied external magnetic field. The authors reported a reduction in blood glucose level of up to 43.8 % in the presence of external magnetic field for 20 hours. However, it was suggested that potential

acute toxicity as well as regulation of the applied magnetic field for long term treatment requires further investigation.

1.6.5 Nanogels (NGs)

Nanogels are nano-range particles from hydrogel family, also termed as hydrogel nanoparticles (Hamidi et al., 2008). These particles show characteristic features of both hydrogels and nanoparticles. As hydrogels, they possess hydrophilicity, swelling capability and biocompatibility (Ranjha et al., 2011, Mudassir and Ranjha, 2008, Ranjha and Mudassir, 2008, Ranjha and Doelker, 1999). Like nanoparticles, they are of nano-size (Patel et al., 2011). Among the numerous classes of nanogels being utilized for oral peptide and protein delivery, only the vinyl and acrylic based nanogels are highlighted in the following discussion.

1.7 Vinyl and acrylic based carriers for oral peptide and protein delivery

There has been great interest in utilizing nanocarriers based on vinyl and acrylic polymers and copolymers in oral peptide and protein delivery. These polymers have been shown to have properties such as muco-adhesive, permeation enhancing and shielding against enzymatic degradation (Bernkop-Schnürch et al., 2003, Bernkop-Schnürch and Clausen, 2002, Tamburic and Craig, 1995). Initially, the Poly(isobutyl cyanoacrylate) (PIBCA) nano-dispersions and poly(alkyl cyanoacrylate) (PACA) nanoparticles were reported for oral delivery of peptide and protein (Graf et al., 2009, Mesiha et al., 2005). Subsequently, pH-responsive delivery system based on vinyl and acrylic polymers were designed. Such nanocarriers were especially beneficial for delivery to the specific region of GIT. The approaches utilizing pH-sensitive characteristics of materials in oral peptide and protein delivery are discussed below:

1.7.1 Polymers possessing pH-dependent swelling behaviour

Researchers have developed pH-sensitive nanocarriers using polymers that exhibit pH-dependent swelling behaviour (Bell and Peppas, 1996). In this context, the poly (methacrylic acid)-poly (ethylene glycol) (PMAA-PEG) co-polymer is widely used to develop pH-sensitive nanocarriers. In acidic environment, these co-polymers remained in collapsed state due to the presence of hydrogen bonds between the carboxylic group of PMMA and oxygen in PEG. However, at basic pH the carboxylic group of PMAA become ionized and swells due to lack of hydrogen bonding and presence of electrostatic repulsion (Bell and Peppas, 1996). Subsequently, pH-sensitive polymethacrylic acid–chitosan–polyethylene glycol (PCP) nanoparticles were developed for oral delivery of proteins such as BSA and insulin. Authors reported good protein encapsulation efficiency (60 to 90 %) and pH responsive in-vitro release profile from PCP nanoparticles (Sajeesh and Sharma, 2006b).

1.7.2 Polymers possessing pH-responsive dissolution characteristics

Co-polymers such as poly (methacrylic acid)-poly ethylacrylate (PMAA-PEA) or poly (methacrylic acid)-poly methacrylate (PMAA-PMA), which pH-responsive dissolution characteristics have been utilized in developing pH-sensitive nanocarriers. These nanocarriers remain in a collapsed state (un-swollen state) at acidic pH, while they are in a swollen state at basic pH (Dai et al., 2000). Eudragit is the most popular example of such polymers. The commercial formulations of Eudragit dissolve at particular pH and therefore are suitable for pH-sensitive delivery to particular region e.g Eudragit[®] L100-55 (consisted of PMAA-PEA) and Eudragit[®] S100 (consisted of PMAA-PMA) which dissolves at pH>5.5 (duodenum) and at pH>7.0 (ileum), respectively. The Eudragit[®] L100-55, S100 and

other co-polymers which are soluble at basic pH have been investigated for oral delivery of peptide and protein therapeutics. These materials serve the purpose of protecting drugs from the acidic environment of the stomach as well as increasing intestinal uptake. Dai et al. (2004) prepared cyclosporine A (CyA) loaded nanoparticles using different pH-sensitive poly (methacrylic acid and methacrylate) copolymers. The authors selected Eudragit[®] E100, Eudragit[®] L100, Eudragit[®] L100-55 and Eudragit[®] S100 as pH-sensitive polymers and studied bioavailability and pharmacokinetics of cyclosporine A (CyA) loaded nanoparticles in Sprague Dawley rats. The entrapped efficiency was approximately 99 % while the particle sizes with various pH-sensitive polymers ranged from 37.4 to 106.7 nm. The authors reported that relative bioavailability of CyA from CyA-S100, CyA-L100-55 and CyA-L100 nanoparticles increased by 32.5%, 15.2 % and 13.6%, respectively.

Zhang et al. (2012) prepared nanoparticles based on thiolated Eudragit L100 for oral insulin delivery. The nanoparticles possessed average size of 308.8 ± 35.7 nm, and loading efficiency (LE%) of $96.4 \pm 0.5\%$. The nanoparticle showed pH dependent *in vitro* release behavior. The circular dichroism (CD) spectroscopy study revealed that the secondary structure of the insulin released from the nanoparticles was preserved.

1.7.3 Vinyl and acrylic based nanogels

pH-sensitive polymers or copolymers were synthesized starting from vinyl and acrylic based monomers or polymers. This approach is advantageous in terms of selecting monomers and obtained nanocarriers with desired pH-sensitive characteristics. The synthesized pH-sensitive nanocarriers are referred to as nanogels. Nanogels based on vinyl and acrylic monomers are of high interest because of their pH-sensitivity and the presence of carboxylic acid functional groups

(Elsaeed et al., 2012, Zha et al., 2011, Wu et al., 2010, Tan et al., 2007). A few examples of vinyl and acrylic monomers are given as follows: 2-hydroxyethyl methacrylate (HEMA), N-isopropylacrylamide (NIPAM), 2-hydroxyethyl methacrylate (HEMA), 2-hydroxypropyl methacrylate (HPMA), oligo(ethylene glycol) monomethyl ether methacrylate (OEOMA), acrylamide (AAm), acrylic acid (AA), methacrylic acid (MAA) and itaconic acid (IA) etc. These synthetic monomers have the added advantages of being cheap, abundant and of reproducible source. In this context, Nayak et al. (2011) prepared pH and temperature sensitive nanogels based on poly-*N*-isopropylacrylamide and acrylic acid (AA) using free radical polymerization. The nanogels were crosslinked using *N*, *N*-methylene bisacrylamide and were pH and temperature sensitive due to the presence of AA and poly-*N*-isopropylacrylamide, respectively. The average size of the nanogels was 150 nm, while nanogels containing only AA showed slightly bigger size of 230 nm. It was suggested that the increase in nanogels size was due to ionization of carboxylic acid functional group of AA. The swelling ratio of nanogels was increased to 1.4 when the pH of the medium was increased from 2.5 to 11.

1.7.4 Nanogels composition and synthesis

The building components of nanogels include synthetic or naturally occurring hydrophilic monomers or polymers. Figure 1.5 illustrates the diversity of nanogels composition based on building components (Mudassir et al., 2015). Nanogels being crosslinked structurally show ability to swell and thus can encapsulate higher amount of drugs. Some nanogels may be responsive to environmental changes such as temperature, pH and magnetic field depending upon building materials. They also show flexibility in adjusting the dose to be administered. Nanogels may be synthesized by association of amphiphilic block polymers with oppositely charged

chain, referred to as nano self-assembly method (Yallapu et al., 2010, Nomura et al., 2005).

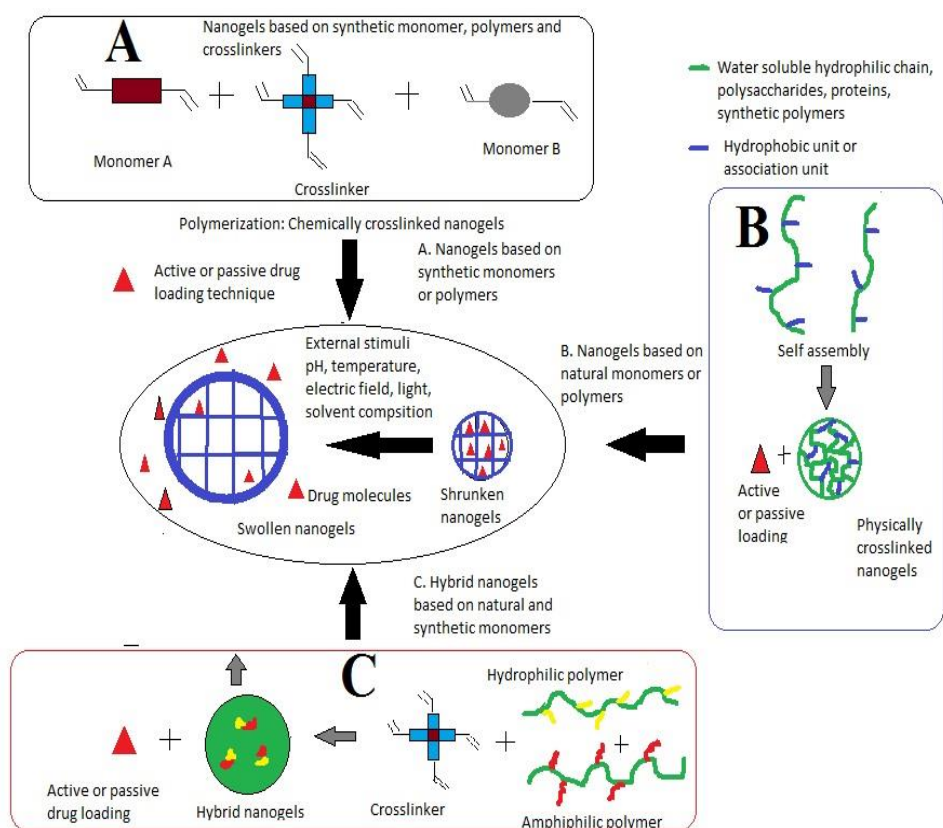


Figure 1.5: Illustrative representation of the diversity of nanogels composition based on building components: (A) nanogels based on synthetic monomers or polymers; (B) based on natural monomers or polymers; (C) hybrid nanogels (Mudassir et al., 2015).

The polymeric nanogels are generally synthesized using polymerization of monomers. Different methods of free radical polymerization which may be involved in nanogels synthesis are described as follows:

1.7.4 (a) Mass polymerization

In mass polymerization, the monomers used are in liquid form. The initiators are dissolved in monomers, hence producing a homogeneous system. Polymerization is initiated via heat or radiation. There are two possible results in mass polymerization. In the first case, the polymer is not soluble in monomers, thus as the polymerization

process proceeds (e.g polymerization of acrylonitrile) a solid polymer is formed through precipitation. In the second case, the obtained polymer is soluble in the monomers. In this case, the viscosity of the polymer and its mass increases until they are converted into solid polymers (e.g. styrene or methyl methacrylate) (Nuyken and Lattermann, 1992).

1.7.4 (b) Solution polymerization

The polymerization is performed by dissolving the monomers in a suitable solvent. Beside that, the synthesized polymer should be dissolved in the selected solvent. The polymer is isolated either by evaporating the solvent or adding excess of non-solvent to precipitate the polymer (Ahmad et al., 1998, Nuyken and Lattermann, 1992).

1.7.4 (c) Suspension polymerization

This process is used for free radical polymerization in which the initiator is first dissolved in monomers, then dispersed in water using a suspending agent. Polymerization takes place in monomer droplets dispersed in the aqueous phase (Nuyken and Lattermann, 1992, Yuan et al., 1991).

1.7.4 (d) Emulsion polymerization

The process of emulsion polymerization is quite similar to suspension polymerization. However, it differs in that the initiator is insoluble in monomers, but soluble in water. In other words, the water insoluble monomers are dispersed in water which also contains initiator and emulsifying agent. Emulsifying agent is dissolved in water and forms a colloidal cluster also known as micelles at higher concentration. Polymerization takes place inside the micelles (Erbil, 2000, Nuyken and Lattermann, 1992).

1.7.5 Mechanism and characteristics of nanogels overcoming barriers to oral peptide and protein delivery

Nanogels possess unique characteristics which may overcome oral peptide and protein delivery barriers. These characteristics include (i) pH sensitive swelling behavior (ii) ability to protect the peptide and protein drugs from the enzymatic degradation and (iii) capability to improve the intestinal permeability by facilitating the opening of intestinal TJs without posing significant toxic effects (Wang et al., 2016, Feng et al., 2014). By possessing these characteristics, the nanogels no longer require separate addition of enzyme inhibitors or permeability enhancers. Furthermore, the nanogels no longer require additional enteric coatings, or filling into the enteric capsules. All the additional processes and incorporation of various chemicals would not only increase the cost of formulation but also pose many questions regarding the toxicity of incorporated materials and stability of the loaded peptide and protein. Figure 1.6 presents schematic diagram of mechanism of pH-sensitive nanogels overcoming the major barriers of oral peptide and protein delivery (Mudassir et al., 2015).

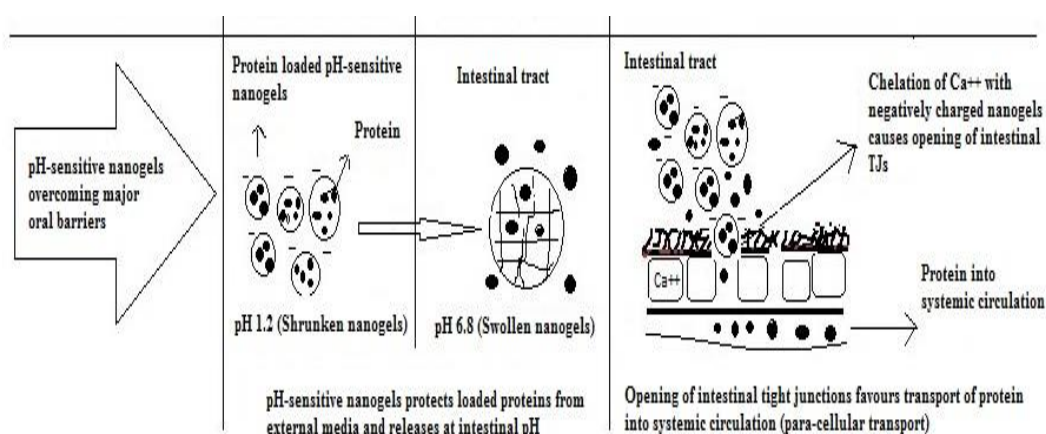


Figure 1.6: Overview of mechanism of pH-sensitive nanogels to overcome major barriers (Mudassir et al., 2015)

1.7.5 (a) pH-sensitive nanogels

The most important characteristic of nanogels in oral peptide and protein delivery is their sensitivity to external pH (Elsaeed et al., 2012, Xiong et al., 2011). The pH-sensitive behaviour of nanogels is due to the presence of certain pH-sensitive functional groups in the polymer chain. The pH sensitive nanogels can be either acidic or basic, which responds to either basic or acidic pH. The acidic functional groups include carboxylic acids (COOH) and sulfonic acids ($-\text{SO}_3$), while the basic groups include primary amines and quaternary ammonium salts (Elsaeed et al., 2012, Xiong et al., 2011). The carboxylic acid functional groups undergo protonation and deprotonation and result in the swelling and de-swelling of the nanogels. At pH below pKa, the carboxylic acid functional groups remain protonated and the network is in a collapsed state. However, above the pKa value, the carboxylic acid functional groups become de-protonated and result in the expansion of networks due to the repulsion of intermolecular charges. The reverse behaviour is observed in primary amine groups and quaternary ammonium salts (Ranjha et al., 2011, Mudassir and Ranjha, 2008, Ranjha and Mudassir, 2008, Ranjha and Doelker, 1999). Figure 1.7 presents the pH sensitive swelling behaviour of carboxylic acid functional groups containing nanogels (Mudassir et al., 2015).